Biophysical Chemistry 162 (2012) 22–34

Contents lists available at SciVerse ScienceDirect

Biophysical Chemistry

journal homepage: http://www.elsevier.com/locate/biophyschem

Dynamics and feedback loops in the transforming growth factor β signaling pathway

Katja Wegner [a,*,1], Anastasia Bachmann [b,1], Jan-Ulrich Schad [c], Philippe Lucarelli [d], Sven Sahle [c], Peter Nickel [d], Christoph Meyer [b], Ursula Klingmüller [d], Steven Dooley [b], Ursula Kummer [c]

[a] Biological and Neural Computation Group, Science and Technology Research Institute, University of Hertfordshire, College Lane, Hatfield, Hertfordshire, United Kingdom
[b] Molecular Alcohol Research in Gastroentorology, Department of Medicine II, Universitätsmedizin Mannheim, University of Heidelberg, Mannheim, Germany
[c] Department for Modeling of Biological Processes, COS Heidelberg and BIOQUANT, University of Heidelberg, Heidelberg, Germany
[d] Systems Biology of Signal Transduction, German Cancer Research Center, Heidelberg, Germany

HIGHLIGHTS

- We present a mathematical model to determine the relevance of feedback loops in the TGF-β signaling.
- Our computational analysis indicated that oscillations are possible under realistic conditions.
- Smad7 and Smurf1/2 have the strongest potential to act as negative feedback regulators.
- Ski, SnoN, SARA, Arkadia have a high potential to also act as positive feedback mechanisms.
- Preliminary experimental data revealed a more dynamic behavior than the simple on-off mechanism.

GRAPHICAL ABSTRACT

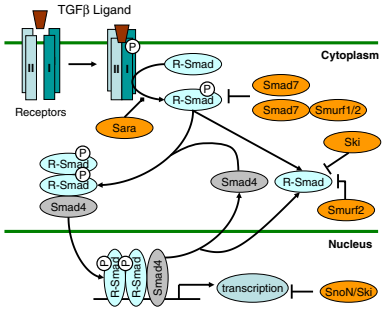

ARTICLE INFO

Article history:
Received 25 October 2011
Received in revised form 19 December 2011
Accepted 20 December 2011
Available online 5 January 2012

Keywords:
Smad signaling
Oscillation
Modeling
Simulation
Negative and positive feedback

ABSTRACT

Transforming growth factor β (TGF-β) ligands activate a signaling cascade with multiple cell context dependent outcomes. Disruption or disturbance leads to variant clinical disorders. To develop strategies for disease intervention, delineation of the pathway in further detail is required. Current theoretical models of this pathway describe production and degradation of signal mediating proteins and signal transduction from the cell surface into the nucleus, whereas feedback loops have not exhaustively been included. In this study we present a mathematical model to determine the relevance of feedback regulators (Arkadia, Smad7, Smurf1, Smurf2, SnoN and Ski) on TGF-β target gene expression and the potential to initiate stable oscillations within a realistic parameter space. We employed massive sampling of the parameters space to pinpoint crucial players for potential oscillations as well as transcriptional product levels. We identified Smad7 and Smurf2 with the highest impact on the dynamics. Based on these findings, we conducted preliminary time course experiments.

1. Introduction

Molecular dissection of signal transduction pathways provides insights into cell responses towards a particular stimulus. Transforming Growth Factor β (TGF-β) family ligands, which comprise e.g. bone morphogenetic proteins (BMPs) and activins, are known as regulators of multiple cellular processes, including immune

* Corresponding author at: Cooperative State University Baden-Wuerttemberg, Erzberger Str. 121, D-76133 Karlsruhe, Germany. Tel.: +49 721 9735 909; fax: +49 721 9735 921.
E-mail addresses: wegner@dhbw-karlsruhe.de (K. Wegner), anastasia.bachmann@medma.uni-heidelberg.de (A. Bachmann).
[1] Contributed equally to this work.

0301-4622/$ – see front matter © 2011 Elsevier B.V. All rights reserved.
doi:10.1016/j.bpc.2011.12.003

suppression, angiogenesis, apoptosis, cell growth and epithelial mesenchymal transition (EMT) [1–3].

Similar to other signaling cascades TGF-β signaling in general procedes via a series of protein activations (e.g. by phosphorylation) and complex formations until a transcription activator translocates into the nucleus where it can influence gene expression. At the same time feedback species are formed which inhibit diverse steps in the signaling pathway.

Specifically, TGF-β initializes signal transduction by binding to the TGF-β receptor type II (TGF-βRII) which recruits the type I receptor (TGF-βRI) leading to its activation by phosphorylation [4]. The activated receptor/ligand complex phosphorylates cytoplasmic receptor-Smads (R-Smads: Smad2 and Smad3) which form homo- or hetero-oligomers with the common-mediator Smad (Co-Smad: Smad4).

R-Smads and Smad4 shuttle continuously between the cytoplasm and the nucleus whereas the R-Smads undergo cycles of receptor-mediated phosphorylation and dephosphorylation [5,6]. Translocation of activated Smad complexes into and their accumulation in the nucleus as well as their interactions with corepressors or coactivators differentially regulates TGF-β target gene expression resulting in the aforementioned context dependent cellular responses [7–9]. Inhibitory Smad7 is activated via a negative feedback loop of the TGF-β pathway by the signaling cascade.

Interaction of activated Smad complexes with corepressors Ski and SnoN leads to repression of the activated complexes, thereby inhibiting Smad dependent target gene expression [10]. Inhibitory Smad7 recruits Smurf1/2 to the active receptor and mediates ubiquitination and degradation of the active receptor-ligand complex [11].

Strength and duration of the TGF-β signal is reflected by the amount of active Smad complexes and their respective target gene transcription rate in the nucleus which is critical for the control of biological responses [5]. Despite detailed knowledge about involved players in TGF-β mediated signal transduction, the mechanisms how information is processed along the pathway is not clear, yet.

Feedback loops generally predominate regulation of and information processing along signaling pathways by determining duration and strength of the signal. In addition, numerous signaling pathways utilize feedback loops as a mechanism for information generation encrypted in e.g. oscillations. Calcium signal transduction is probably the best studied example for information processing in oscillations [12–14]. In hepatocytes for example, the frequency of calcium oscillations contains the information about the strength of the stimulus, whereas the shape of the amplitude encodes information about the kind of stimulus (for a review see [15]). Furthermore, cAMP [16], NFκB [17], and MAPK [18] have been shown to oscillate under a number of circumstances for information processing.

Mathematical modeling was employed to study and understand the biochemical mechanisms underlying these oscillations and to get more insights into the nature of information transfer in the respective systems, e.g. determination of transcriptional outcome [19–21].

To understand factors that influence the information processing in the TGF-β signal transduction pathway we developed a detailed mathematical model to determine the influence of feedback loops on the dynamics in the signaling. Moreover, it was reported that BMP, one member of the TGF-β super family, induces oscillations in the range of one to two hours which has been shown in mRNA and protein concentration measurements of receptor-regulated and inhibitory Smads [22]. Therefore, we also analyze the potential of TGF-β signaling to display oscillatory dynamics and the likely range of frequencies expected.

The mathematical models currently published for the TGF-β signaling pathway are far from describing feedback loops and their influence on dynamics of the pathway. Vilar et al. [23] developed a model comprising ligand binding, receptor complexes formation and degradation. The main focus of the models of Clarke and coworkers [24] and Melke and colleagues [25] was R-Smad phosphorylation, complex formation with Co-Smads and translocation into the nucleus. The latter model additionally includes Smad7 inhibiting active receptor complexes. Zi and Klipp [26] combined these models [23–25], while Schmierer et al. [27] presented a model describing Smad (de)phosphorylation, mainly focusing on the shuttling of the Smads between cytoplasm and nucleus. Additionally, Zi et al. recently published the sensitivity of the signal activity according to ligand doses at different time scales [28]. Although these models are helpful, they lack the integration of the several feedback mechanisms, an indispensable requirement to understand information processing along the TGF-β signaling cascade.

In the present article, we set up a new model for the TGF-β signaling pathway by including:

- formation of receptor complexes,
- recruitment and phosphorylation of R-Smads (Smad2 and Smad3) as well as formation of active Smad complexes with Co-Smads (Smad4),
- shuttling between cytoplasm and nucleus, and
- feedback loops including Arkadia, Smad7, Smurf1, Smurf2, SnoN and Ski.

With the present redefined model we predicted the impact of feedback loops on the concentration of transcriptionally active Smad complexes, target gene transcription and on whether or not the pathway exhibits oscillations within a realistic range of parameters. In addition, we investigated likely periods of the oscillation to guide experimental investigations.

The suggested narrow time point sampling with different TGF-β concentrations revealed experimental data with a more dynamic behavior of the pathway than the simple on-off mechanism outlined in current literature [29,5] and in existing computational models [23–25].

2. Material and methods

2.1. Computational approaches

The model is represented by a set of ordinary differential equations (ODEs) which are listed in the supplement. Simulations were performed by numerical integration of the ODEs using Copasi [30]. Steady-state calculations, optimization, sensitivity analysis and random sampling were also done with Copasi.

2.2. Experimental approaches

2.2.1. Reagents

Recombinant TGF-β1, Peprotech (Hamburg, Germany) or R&D Systems GmbH (Wiesbaden, Germany), used as indicated. Transfection reagents RNAiMAX, Invitrogen (Karlsruhe, Germany) and Lipofectamine 2000, Invitrogen (Karlsruhe, Germany); siRNA, Qiagen, (Hilden, Germany); Ad(CAGA)9-MLP-Luc was described previously [31–33]; AdGFP was used as control. An MOI of 100 was used for infection with Ad(CAGA)9-MLP-Luc and AdGFP. Antibodies used: anti-Smad2/3 (Cell Signaling Technology, Boston, USA), pSmad2, pSmad3 (Cell Signaling), β-actin (Sigma), SARA (SantaCruz Biotechnology, Santa Cruz, USA). Horseradish peroxidase-linked secondary antibodies were either from SantaCruz or GE Healthcare (München, Germany).

2.2.2. Isolation of primary hepatocytes

Mouse hepatocytes were isolated by a two step collagenase perfusion procedure from 6 to 12 week old male C57BL/6 mice (Charles River) [34]. The use of mice for hepatocyte isolation has been approved by the animal care committees. Animals were handled and housed according to specific pathogen free (SPF) conditions.

2.2.3. Cell culture

Non-differentiated AML12 mouse hepatoma cells were obtained from American Type Cell Culture Collection (ATCC). Cells were grown in F-12/DMEM complete medium (Invitrogen, Karlsruhe, Germany) and were plated at a density of 3×10^5 in 6-well plates, starved over night with 0% FBS medium before human TGF-β (1 ng/ml) (Peprotech, London, UK) was added.

Primary hepatocytes were seeded and cultured with a density of 2×10^6 in 2 ml full medium (phenol red-free Williams E medium (Biochrom)) supplemented with 10% (v/v) FBS (Invitrogen), 1 mM dexamethasone, 10 mg/ml insulin, 2 mM L-glutamine, and 1% (v/v) penicillin/streptomycin 100x (both Invitrogen) using collagen I-coated 6 cm dishes (BD Biosciences) at 37 °C, 5% CO_2 and 95% humified atmosphere. After 4 h cells were washed with PBS (PAN Biotech) to remove unattached hepatocytes and subsequently cultured in cultivation medium (phenol red-free Williams E medium supplemented with 1 mM dexamethasone, 2 mM L-glutamine, and 1% (v/v) penicillin/streptomycin 100x) over night. 4 h prior conducting the experiment, hepatocytes were starved for 4 h in reduced medium (phenol red-free Williams E medium supplemented with 2 mM L-glutamine, and 1% (v/v) penicillin/streptomycin 100x). For stimulation experiments of hepatocytes 1 ng/ml recombinant human TGF-β1 (R&D Systems GmbH, Wiesbaden, Germany) was used.

2.2.4. Transient transfection

AML12 cells were seeded in 12 well plates and transfected using Lipofectamine 2000 (Invitrogen, Karlsruhe, Germany) according to manufacturers' instructions. Plasmids were obtained from Addgene (Cambridge, USA), wtSARA (Addgene plasmid 11738) and SARA dSBD (Addgene plasmid 11737) lacking the Smad binding domain. TGF-β stimulation experiments were conducted 16 h post transfection.

2.2.5. Adenovirus preparation, quantification and infection

Adenovirus vectors were expanded, purified and quantified as described [35]. AML12 cells were seeded with a density of 1×10^5 in 12-well plates. 2 h after Adenoviral infection, cells were washed 3 times with HBBS and incubated over night in serum free F12/DMEM medium as indicated under cell culture conditions.

2.2.6. siRNA knock down

AML12 cells were seeded in 24-well plates and transfected with siRNA against SARA (5′-AACAATGGAAATAATAGTAAA-3′) and AllStars RNAi control from Qiagen (Qiagen, Hilden, Germany) with RNAiMax (Invitrogen, Karlsruhe, Germany) due to manufacture's instruction.

2.2.7. Luciferase reporter assay

For luciferase reporter assays, AdCAGA9-MLP-Luc was used [31,32]. Luciferase activity was measured with Steady-Glo Luciferase (Promega, Mannheim, Germany) as described [33]. Luminometric measurements were performed using either Tecan infinite M200 or Thermo Luminoskan Ascent (Thermo Fisher, Schwerte, Germany). Obtained values (Unit D relative light units, RLU) were normalized to protein content. Results presented are means ± SE of three independent experiments.

For immunoprecipitation, whole cell lysates of primary hepatocytes were prepared with RIPA buffer, supplemented with protease and phosphatase inhibitors. Lysates were rotated for 20 min at 4 °C and sonicated for 30 s (Sonopuls, Bandelin). Following centrifugation for 10 min at 14,000 rpm and 4 °C, supernatants were collected and incubated with anti-Smad2/3 antibody over night (diluted 1:1000, Cell Signaling). Immunoprecipitated proteins were separated by SDS-PAGE and immunoblotting was performed with anti-Smad2/3 (diluted 1:1000) and anti-pSmad2 (diluted 1:1000, Cell Signaling). Horseradish peroxidase conjugated secondary antibodies (GE Healthcare) were used for chemiluminescence detection employing ECL or ECL Advance substrate (GE Healthcare). Signal quantification was performed using a LumiImager system (Roche Diagnostics) as described before [36].

3. Results

3.1. Mathematical model of the TGF-β signaling pathway

The outcome of signal transduction in biological systems is determined by events in different cellular compartments. In the present model of TGF-β signaling we implemented the main cellular localizations of reactions, the cytoplasm and the nucleus. The model consists of 91 reactions as well as 53 species in two compartments and will be available on Biomodels.net [37]. We selected mass action kinetics to describe most of the investigated reactions, whereas phosphorylation and dephosphorylation events of Smad proteins are described by Michaelis-Menten-type kinetics. Mass action kinetics are appropriate for complex formation and other non-enzymatic events. Its use for complex/protein degradation, however, is a simplification. A graphical representation of the model is shown in Fig. 1 and the reactions are displayed in Table 1, whereas related kinetics and parameters are shown in Table 2. The differential equations can be found in the supplementary material.

The receptor complex is formed at the cell membrane and is initialized by ligand binding to the TGF-β-RII (Table 1 reaction 5), which recruits TGF-β-RI (Table 1 reaction 6). Type I and type II receptors are synthesized and degraded (Table 1 reactions 1–4), whereas the active receptor complex is either degraded (Table 1 reactions 7 + 25) or recycled (Table 1 reactions 6 + 8).

The active receptor complex recruits and phosphorylates cytoplasmic R-Smads, Smad2 and Smad3 (Table 1 reaction 11) [4]. Smad2 and Smad3 are structurally similar (92% identity at the amino-acid sequence level [38]) and according to current knowledge both take part in similar reactions during TGF-β downstream signaling. Variations in the biological outcome are cell type/context dependent and arise in the nucleus, where Smad2 and Smad3 have distinct affinities to transcriptional co-regulators and interact with different transcription factors to regulate the transcription of target genes [39]. In contrast to the simplified scheme in Fig. 1 and in Table 1, in the present model Smad2 and Smad3 as well as Smurf1, Smurf2, Ski and SnoN are treated as independent components (variables).

Constitutive expression of components is implemented in the model with constant production rates and linear degradation rates (e.g. Table 1: reactions 9, 10), while the production of feedback species is dependent on gene activation by Smad complexes (e.g. Table 1: reactions 22). In addition to the linear degradation rate, R-Smads are degraded upon ubiquitination — in the case of Smad2 this process is Smurf2 dependent (Table 1: reaction 40). Phosphorylated R-Smads (pRSmads) homo- or hetero-oligomerize [40,41] with Co-Smad4 (Table 1: reactions 16–18), translocate to the nucleus and bind to transcription factors and specific promoter sites [42]. The exact composition of these active Smad complexes is still under debate and may vary cell type and context dependent [39]. Since phosphorylated R-Smads preferentially form hetero-oligomers, which are also more efficient than homo-oligomers [41,43,27], we did not integrate the formation of homo-oligomers into the model. The stoichiometry of this reaction can easily be adjusted to create other compositions, if necessary.

Binding of Smad4 to phosphorylated R-Smads and formation of active Smad complexes occurs in the cytoplasm (Table 1: reaction 18) as well as in the nucleus (Table 1: reaction 41) [4]. The cytoplasmic complexes translocate to the nucleus with similar rates as (un) phosphorylated Smads [43,44] (Table 1: reaction 35). All active Smad complexes and phosphorylated R-Smads are retained in the nucleus until R-Smads are dephosphorylated by nuclear phosphatases PPM1A/PP2Ca [45], which then results in release of Smad4 (Table 1: reactions 43, 44) [4,5]. Only monomeric unphosphorylated

R-Smads and Smad4 translocate back to the cytoplasm [43] (Table 1: reactions 32, 34) and re-enter the cycle of phosphorylation, complex formation, translocation and dephosphorylation as long as the TGF-β receptors remain active [4].

The Smad anchor for receptor activation (SARA) (Table 1: reactions 12, 13) recruits R-Smads and presents them to the active ligand-receptor complex (Table 1: reactions 14, 15) [46] in the EEA1 endosome, where SARA is located [47]. Phosphorylation of SARA-bound Smads decreases their binding affinity to SARA and causes their release [48,40]. It is controversially discussed in the literature whether the interaction with SARA is required for Smad C-terminal phosphorylation [49,50] or not [51,52].

Due to simplifications, the reactions involving SARA occur in the cytoplasm in the present mode. The decision not to integrate SARA interaction in further detail is based on experimental results from AML12 cells, as described in the section Experimental results.

Since the release of SARA is induced by receptor-mediated Smad phosphorylation [46], the production rate for SARA increases with the concentration of formed Smad complexes, reflecting the strength of the TGF-β signal (Table 2: reaction 12). The same rate law is

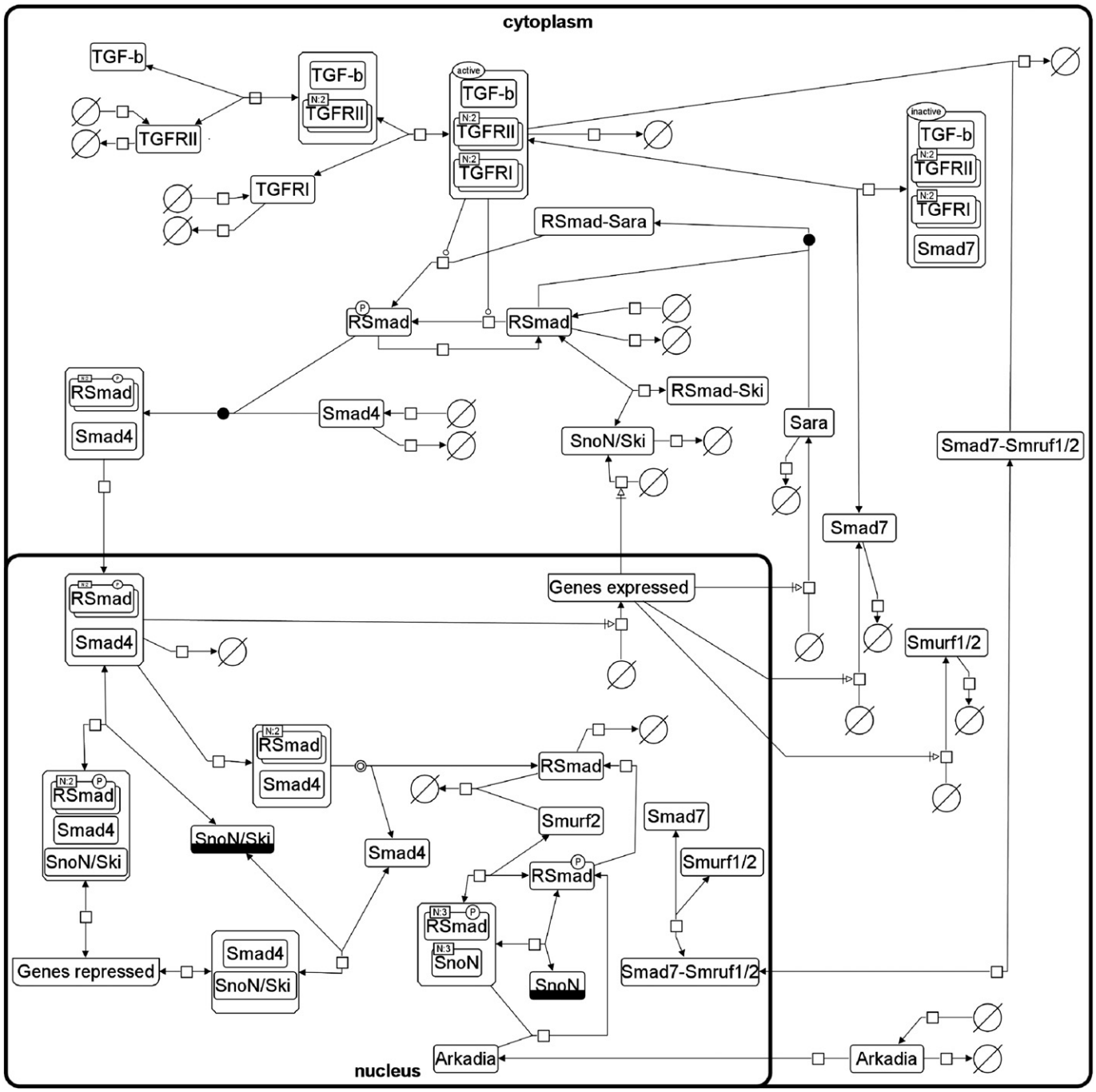

Fig. 1. A graphical overview of main reactions and feedback loops in the presented model of TGF-β signaling as SBGN map [83]. Most transport reactions as well as formation of Smad complexes in the nucleus are excluded from the map to reduce complexity. All reactions with glyphs that are named by two proteins are represented as two single reactions in the model.

Table 1
Reaction equations and the used rate laws. Note, equations with R-Smad represent two different reactions in the model, since Smad2 or Smad3 were included as separate variables. The same holds for Ski/SnoN and Smurf1/2.

	Reaction	Description	Rate law
Cytoplasm			
1	$\rightarrow TGF\beta RI$	Input	Constant flux
2	$\rightarrow TGF\beta RII$	Input	Constant flux
3	$TGF\beta RI \rightarrow$	Degradation	Mass action
4	$TGF\beta RII \rightarrow$	Degradation	Mass action
5	$2TGF\beta RII \rightarrow TGF\beta\_TGF\beta RII$	Ligand binding	Own rate law
6	$TGF\beta\_TGF\beta RII + 2TGF\beta RI \leftrightarrow Rec_{act}$	Receptor complex	Mass action
7	$Rec_{act} \rightarrow$	Degradation	Mass action
8	$TGF\beta\_TGF\beta RII \rightarrow 2TGF\beta RII$	Receptor recycling	Mass action
9	$\rightarrow RSmad_c$	Input	Constant flux
10	$RSmad_c \rightarrow$	Degradation	Mass action
11	$RSmad_c \rightarrow pRSmad_c$	Phosphorylation	Michaelis-Menten
12	$\rightarrow$ SARA	Input	Own rate law
13	$SARA \rightarrow$	Degradation	Mass action
14	$RSmad_c + SARA \leftrightarrow RSmad\_SARA$	Binding	Mass action
15	$RSmad\_SARA \rightarrow pRSmad_c + SARA$	Phosphorylation	Own rate law
16	$\rightarrow Smad4_c$	Input	Constant flux
17	$Smad4_c \rightarrow$	Degradation	Mass action
18	$2pRSmad_c + Smad4_c \rightarrow pRSmad\_Smad4_c$	Complex	Mass action
19	$\rightarrow Smad7_c$	Input	Own rate law
20	$Smad7_c + Rec_{act} \leftrightarrow Rec\_Smad7$	Inhibition	Mass action
21	$Smad7_c \rightarrow$	Degradation	Mass action
22	$\rightarrow Smurf1/2_c$	Input	Own rate law
23	$Smurf1/2_c \rightarrow$	Degradation	Own rate law
24	$pRSmad_c \rightarrow RSmad_c$	Dephosphorylation	Own rate law
25	$Rec_{act} + Smad7\_Smurf1/2_c \rightarrow$	Degradation	Mass action
26	$\rightarrow SnoN/Ski$	Input	Own rate law
27	$SnoN/Ski \rightarrow$	Degradation	Mass action
28	$RSmad_c + Ski \leftrightarrow RSmad\_Ski_c$	Inhibition	Mass action
29	$\rightarrow Arkadia_c$	Input	Mass action
30	$Arkadia_c \rightarrow$	Degradation	Mass action
Transport			
31	$Arkadia_c \rightarrow Arkadia_n$		Mass action
32	$RSmad_c \leftrightarrow RSmad_n$		Mass action
33	$pRSmad_c \rightarrow pRSmad_n$		Mass action
34	$Smad4_c \leftrightarrow Smad4_n$		Mass action
35	$pRSmad\_Smad4_c \rightarrow pRSmad\_Smad4_n$		Mass action
36	$Smad7_c \leftrightarrow Smad7_n$		Mass action
37	$Smad7\_Smurf1/2_c \leftrightarrow Smad7\_Smurf1/2_n$		Mass action
38	$Smurf1/2_c \leftrightarrow Smurf1/2_n$		Mass action
39	$SnoN/Ski_c \leftrightarrow SnoN/Ski_n$		Mass action
Nucleus			
40	$Smad2_n + Smurf2_n \rightarrow$	Degradation	Mass action
41	$2pRSmad_n + Smad4_n \rightarrow pRSmad\_Smad4_n$	Complex	Mass action
42	$pRSmad_n \rightarrow RSmad_n$	Dephosphorylation	Own rate law
43	$pRSmad\_Smad4_n \rightarrow RSmad\_Smad4_n$	Dephosphorylation	Michaelis-Menten
44	$RSmad\_Smad4_n \rightarrow 2RSmad_n + Smad4_n$	Dissociation	Mass action
45	$pRSmad\_Smad4_n + 2SnoN/Ski_n \leftrightarrow pRSmad\_Smad4\_SnoN/Ski_n$	Inhibition	Mass action
46	$pRSmad\_SnoN_n + Smurf2_n \rightarrow pRSmad_n$	Degradation of SnoN	Mass action
47	$Smad4_n + SnoN/Ski_n \leftrightarrow Smad4\_SnoN/Ski_n$	Inhibition	Mass action
48	$Smad7_n + Smurf1/2_n \leftrightarrow Smad7\_Smurf1/2_n$	Complex	Mass action
49	$Smad3_n \rightarrow$	Degradation	Mass action
50	$pRSmad\_Smad4_n + freePromoters \leftrightarrow geneProduct$	Transcription	Mass action
51	$pRSmad\_Smad4\_SnoN/Ski_n + freePromoters \leftrightarrow inactivePromoters$	Repression	Mass action
52	$Smad4\_SnoN/Ski_n + freePromoters \leftrightarrow inactivePromoters$	Repression	Mass action
53	$pRSmad_n + SnoN_n \rightarrow pRSmad\_SnoN_n$	Complex	Mass action
54	$pRSmad\_SnoN_n + Arkadia_n \rightarrow pRSmad_n$	Degradation	Mass action
55	$pRSmad\_Smad4_n \rightarrow$	Degradation	Mass action

defined for the production of Ski, SnoN, Smurf1 and Smurf2, which are all induced by the TGF-β signaling pathway (Table 2: reaction 22, 26).

One important feature of signal transduction processes in biological systems, to guarantee the ability to respond to a novel stimulation and to keep the pathway functional, is time limitation of activity. Shutting off signal transduction is achieved via inhibitory pathways, which are in general induced by negative feedback mechanisms. Therefore, the following negative feedback loops were implemented into the model:

- induction of Smad7
- Smurf-Smad7 axis
- Ski-SnoN axis
- Arkadia

Active Smad complexes in the nucleus induce the expression of Smad7 (I-Smad) [53,32] (Table 1: reactions 19, 21) which binds to the active ligand-receptor complex, thereby blocking binding and phosphorylation of cytoplasmic R-Smads (Table 1: reaction 20) [54,55]. The Smad4-SnoN complex (Table 1: reaction 47) is binding to the Smad7 promoter and blocks expression of Smad7 [56] (this is incorporated into the rate law of reaction 19 in Table 2).

Smurf1 and Smurf2 are located in the nucleus and the cytoplasm (Table 1: reactions 22, 23) [11]. Both are, like Smad7, induced by TGF-β signaling for feedback regulation of the pathway (Table 2: reaction 22). In the nucleus Smurf1 and Smurf2 form complexes with Smad7 (Table 1: reaction 48). Thereafter, the complexes move to the plasma membrane (Table 1: reaction 37) and target active receptor-ligand complexes for degradation (Table 1: reaction 25) [11,57]. Another part of the Smurf-Smad7 axis in the negative regulation of the TGF-β signaling is, that the concentration of Smad7 enhances the auto-ubiquitination of Smurf2 [58] (this is incorporated into the rate law of reaction 23 in Table 1), while Smurf2 supports the degradation of unphosphorylated Smad2 via the proteasome (Table 1: reaction 40) [59].

Ski and SnoN (Table 1: reactions 26, 27), both members of the Ski family [60,61] are nuclear co-repressors and are part of the Ski-SnoN negative feedback loop, bind to the same DNA sequence like active Smad complexes, thus preventing Smad dependent target gene expression (Table 1: 45, 51) [61,10]. Since this competitive binding is the single inhibitory mechanism described for the Ski-SnoN feedback loop at the DNA level, we assume that the Smad complex is inactive if SnoN or Ski is bound to DNA and is active after their dissociation. If SnoN binds to the phosphorylated R-Smads (Table 1, reaction 53) [62], the R-Smads can recruit Smurf2 which will degrade SnoN (Table 1, reaction 46) [63]. Ski and SnoN can also bind to Smad4 only (Table 1: reaction 47) [60], e.g. to repress expression of Smad7 (Table 1: reaction 19) [64]. Complexes with Ski/SnoN and other transcription factors may in addition bind to the DNA in competition with transcriptionally active Smad complexes, thereby preventing gene expression.

The last negative feedback loop of TGF-β signaling in the present model is controlled by Arkadia [65–67], which degrades Ski/SnoN bound to phosphorylated R-Smads in the nucleus (Table 1: reaction 54) and physically interacts with Smad7, thus targeting it for ubiquitination and degradation (Table 1: reaction 21).

Based on the above knowledge, we added several transport mechanisms in the present model to exchange components (shuttling of Arkadia, R-Smad, Smad4, Smad7, Ski, SnoN, Smurf1 and Smurf2) between the cytoplasm and the nucleus (Table 1: reactions 31–39), whereby transport of the (phosphorylated) R-Smads, Smad4, and the active complexes are independent from each other (Table 1: reactions 33–35) [5].

The reactions 50–52 in Table 1 describe in a simplified way the binding of active and repressor complexes to target promoter sites in TGF-β responsive genes.

Table 2
Mathematical representation of each reaction, including parameters as available in the literature. If a parameter value differs from the literature value, the literature value is shown next to the reference. Parameters which are not from literature were estimated. This set of parameters is used for Fig. 2. Units used: min, l and μmol.

rct	Function	Parameters	Reference
1	$f_1 = v_1$	$v_1 = 0.0125$	0.125 [23]
2	$f_2 = v_2$	$v_2 = 0.00146$	0.25 [23]
3	$f_3 = k_3[TGF\beta RI]$	$k_3 = 0.027778$	[23]
4	$f_4 = k_4[TGF\beta RII]$	$k_4 = 0.027778$	[23]
5	$f_5 = k_5[TGF\beta RII]^2[TGF\beta]$	$k_5 = 9.45$	
6	$f_6 = k_6[TGF\beta\_TGF\beta RII][TGF\beta RI]^2 - k_{-6}[Rec_{act}]$	$k_{6/-6} = 0.03333$	[23]
7	$f_7 = k_7[Rec_{act}]$	$k_7 = 0.027778$	[23]
8	$f_8 = k_8[TGF\beta\_TGF\beta RII]$	$k_8 = 0.033333$	[23]
9	$f_9 = v_9$	$v_{9Smad2} = 0.0156$, $v_{9Smad3} = 0.04528$	
10	$f_{10} = k_{10}[RSmad_c]$	$k_{10} = 0.2$	
11	$f_{11} = \frac{k_{11}[Rec_{act}][RSmad_c]}{K_{m_{11}} + [RSmad_c]}$	$k_{11} = 1000$, $K_{m_{11}} = 0.0318$	
12	$f_{12} = v_{12} + k_{12}[geneProduct]$	$v_{12} = 0.0001$, $k_{12} = 0.031$	
13	$f_{13} = k_{13}[SARA]$	$k_{13} = 0.065$	
14	$f_{14} = k_{14}[RSmad_c][SARA] - k_{-14}[RSmad_{Sara}]$	$k_{14} = 1, k_{-14} = 0.1$	
15	$f_{15} = \frac{k_{15}[Rec_{act}][RSmad_{Sara}]}{K_{m_{15}} + [RSmad_{Sara}]}$	$k_{15} = 3.51$, $K_{m_{15}} = 0.53$	[24]
16	$f_{16} = v_{16}$	$v_{16} = 0.01183$	
17	$f_{17} = k_{17}[Smad4_c]$	$k_{17} = 0.1266$	
18	$f_{18} = k_{18}[pRSmad_c]^2[Smad4_c]$	$k_{18} = 1000$	
19	$f_{19} = \frac{v_{19} + k_{19}[geneProduct]}{1 + [Smad4_{SnoN}] + [Smad4_{Ski}]}$	$v_{19} = 0.0001$, $k_{19} = 0.1$	
20	$f_{20} = k_{20}[Smad7_c][Rec_{act}] - k_{-20}[Rec\_Smad7]$	$k_{20} = 8.69$, $k_{-20} = 0.01$	
21	$f_{21} = k_{21}[Smad7](1 + [Arkadia])$	$k_{21} = 0.1$	
22	$f_{22} = v_{22} + k_{22}[geneProduct]$	$v_{22Sm1} = 0.0001$, $k_{22Sm1} = 0.0022$, $v_{22Sm2} = 0.000228$, $k_{22Sm2} = 0.00285$	
23	$f_{23} = k_{23}[Smurf1/2](1 + [Smad7_c])$	$k_{23Sm1} = 0.5$, $k_{23Sm2} = 0.05$	
24	$f_{24} = \frac{V_{24}[pRSmad_c]}{K_{m_{24}} + [pRSmad_c]}$	$V_{24} = 0.53$, $K_{m_{24}} = 3.51$	[24]
25	$f_{25} = k_{25}[Rec_{act}][Smad7\_Smurf1/2_c]$	$k_{25} = 1900$	
26	$f_{26} = v_{26} + k_{26}[geneProduct]$	$v_{26} = 0.00002$, $k_{26} = 0.00055$	
27	$f_{27} = k_{27}[SnoN/Ski_c]$	$k_{27} = 0.232$	
28	$f_{28} = k_{28}[RSmad_c][Ski_c] - k_{-28}[RSmad\_Ski_c]$	$k_{28/-28} = 0.1$	
29	$f_{29} = v_{29}$	$v_{29} = 0.00002$	
30	$f_{30} = k_{30}[Arkadia_c]$	$k_{30} = 0.1$	
31	$f_{31} = k_{31}[Arkadia_c] - k_{-31}[Arkadia_n]$	$k_{31} = 0.1$, $k_{-31} = 0.1$	[24]
32	$f_{32} = k_{32}[RSmad_c] - k_{-32}[RSmad_n]$	$k_{32} = 0.156$, $k_{-32} = 0.336$	[86]
33	$f_{33} = k_{33}[pRSmad_c]$	$k_{33} = 16.6$	[24]
34	$f_{34} = k_{34}[Smad4_c] - k_{-34}[Smad4_n]$	$k_{34/-34} = 0.156$	[86]
35	$f_{35} = k_{35}[pRSmad\_Smad4_c]$	$k_{35} = 0.16$	[26]
36	$f_{36} = k_{36}[Smad7_c] - k_{-36}[Smad7_n]$	$k_{36} = 0.1$, $k_{-36} = 0.01$	
37	$f_{37} = k_{37}[Smad7\_Smurf1/2_c] - k_{-37}[Smad7\_Smurf1/2_n]$	$k_{37} = 1, k_{-37} = 0.01$	
38	$f_{38} = k_{38}[Smurf1/2_c] - k_{-1}[Smurf1/2_n]$	$k_{38Sm1} = 0.05$, $k_{-38Sm1} = 3$, $k_{38Sm2} = 0.2333$, $k_{-38Sm2} = 1.8056$	
39	$f_{39} = k_{39}[SnoN/Ski_c] - k_{-39}[SnoN/Ski_n]$	$k_{39} = 0.1, k_{-39} = 0.2$	
40	$f_{40} = k_{40}[Smad2_n][Smurf2_n]$	$k_{40} = 0.2$	
41	$f_{41} = k_{41}[pRSmad_n]^2[Smad4_n]$	$k_{41} = 255.068$	
42	$f_{42} = \frac{V_{42}[pRSmad_n]}{K_{m_{42}} + [pRSmad_n]}$	$V_{42} = 3.51$, $K_{m_{42}} = 0.53$	[24]
43	$f_{43} = \frac{V_{43}[pSmad_{Smad4n}]}{K_{m_{43}} + [pSmad_{Smad4n}]}$	$V_{43} = 2.34$, $K_{m_{43}} = 40$	
44	$f_{44} = k_{44}[RSmad\_Smad4]$	$k_{44} = 0.0492$	[24]
45	$f_{45} = k_{45}[pRSmad\_Smad4_n][SnoN/Ski_n]^2 - k_{-45}[pRSmad\_Smad4\_SnoN/Ski_n]$	$k_{45/-45} = 1.6$	[90]
46	$f_{46} = k_{46}[pRSmad\_SnoN_n][Smurf2]$	$k_{46} = 0.232$	
47	$f_{47} = k_{47}[Smad4_n][SnoN/Ski] - k_{-47}[Smad4\_SnoN/Ski_n]$	$k_{47} = 1$, $k_{-44} = 0.05288$	
48	$f_{48} = k_{48}[Smad7_n][Smurf1/2_n] - k_{-48}[Smad7\_Smurf1/2_n]$	$k_{48} = 2.9, k_{-48} = 0.2$	
49	$f_{49} = k_{49}[RSmad_n]$	$k_{49} = 0.2$	
50	$f_{50} = k_{50}[pRSmad\_Smad4_n][freePromoters] - k_{-50}[geneProduct]$	$k_{50} = 0.463$, $k_{-50} = 0.102$	
51	$f_{51} = k_{51}[pRSmad\_Smad4\_SnoN/Ski_n] \cdot [freePromoters] - k_{-51}[inactivePromoters]$	$k_{51/-51} = 0.2$	
52	$f_{52} = k_{52}[Smad4\_SnoN/Ski_n][freePromoters] - k_{-52}[inactivePromoters]$	$k_{52/-52} = 0.2$	
53	$f_{53} = k_{53}[pRSmad_n]^3[SnoN_n]^3 - k_{-53}[pRSmad\_SnoN_n]$	$k_{53/-53} = 1$	[90]
54	$f_{54} = k_{54}[pRSmad\_SnoN_n][Arkadia_n]^3$	$k_{54} = 0.1$	
55	$f_{55} = k_{55}[pRSmad\_Smad4_n]$	$k_{55} = 0.005$	

3.2. Analysis of feedback loops

To understand which factors participate in information processing and have impact on time course of TGF-β signaling, we investigated a) if and how this signaling pathway can give rise to oscillations and b) how the steady-state levels of the transcriptionally active Smad-complex as well as gene products depend on regulation of this pathway, i.e. feedback loops in the system.

To identify oscillating behavior of TGF-β Smad signaling within a realistic parameter range, we used global optimization algorithms. The basic idea of optimization is to maximize a (heuristically defined) target function for which the value will be large if the simulation has oscillatory behavior. The target function is defined by the integral over time of the absolute rate change values of one species in the model over time. This integral quantifies concentration changes in either direction during simulation time. If the concentration changes a lot in relation to its average value, this may indicate oscillations. A diagram exemplifying this approach can be found in the supplement. This is only a heuristic measure since a single very large peak could result in a large absolute concentration change in relation to its end value. However, this is unlikely to occur since we start integration of the change after some time (when transients have settled) and we integrate over a long period of time (so that even small oscillations could add up to more absolute change than one single large peak). This leads to the target function

$$f = \frac{r}{c} \tag{1}$$

where r is the integral of the absolute value of the rate of change of one of the species and c denotes the average concentration.

This target function would be maximized using a global optimization algorithm. A problem with this is that this function can be maximized either by increasing the change or by decreasing the average concentration to very small values. To avoid the latter we use the following target function

$$f = \frac{r + r \cdot c}{1 + c + c^2} \tag{2}$$

where r and c are defined as above. This function behaves like r/c for large c but approaches r for small values of c, while being monotonous in between. We used the global optimization routines particle swarm [68], genetic algorithm [69] and evolutionary strategies [70] to optimize this function and find oscillations. These optimizers are based on different strategies. To increase the likelihood for finding the optimum, we applied each of them.

Default parameters as implemented in Copasi were used for the optimization (e.g. particle swarm: swarm size 50, std. deviation 1e-06; genetic algorithm and evolutionary strategies: population size 20).

Global optimizers were used since we allowed the variation of basically all parameters in the system creating a high-dimensional parameter space. Whenever experimental data were available (see Table 2), parameters were allowed to be varied by 20%. If no data were available, starting with the values depicted in Table 2 all parameters were varied within a range from two orders of magnitude below the starting value to three orders of magnitude above the starting value. We additionally performed this analysis with even broader (ranging seven orders of magnitude), as well as with a more narrow range (ranging four orders of magnitude). In all cases, the results were qualitatively the same.

Within these boundaries, large oscillatory regimes were found with periods between ca. 30 min and 2 h (an example time series is displayed in Fig. 2). We analyzed the impact of the different parameters on frequency and amplitude of the displayed oscillations. This was achieved by a sensitivity analysis computing the variation of the frequency or amplitude caused by small perturbations of the respective parameters. Only few parameters strongly influence the frequency of the oscillations (with the parameter set displayed in Fig. 2). These are parameters leading to the production or degradation of Smad7 or the two receptor species. More parameters are influencing the amplitude. This is no surprise, since the displayed parameter set is relatively close to the Hopf bifurcation. In addition to the parameters influencing the frequency, here parameters involved in the production and degradation of Smad4 and RSmads, in the transport and dephosphorylation of RSmads and in the transcription process are prevalent.

To investigate which feedback loops are mainly responsible for the observed behavior we manually varied parameters for the production of the different feedback components (Arkadia, Smad7, Smurf1, Smurf2, Ski, SnoN and SARA) starting at the values used for the time series in Fig. 2. For the selected oscillatory regime, oscillations are retained when the productions for SARA, Ski, SnoN and Smurf1 are decreased to zero, while Smurf2 and Smad7 have a major impact and cannot be abrogated.

However, to gain a more general picture of the impact of the different feedback species on the potential oscillatory dynamics, we had to investigate a larger part of the parameter space which is manually not possible. Therefore, we used the optimization procedures described above, whereas knocking out one feedback species at a time. Apart from the species listed above, the knock out of Smad7 or Smurf2 still results in oscillations in different places in parameter space, while some species display high, unphysiological concentrations (e.g. Smad4).

Finally, we could not achieve stable oscillatory behavior with our approach when knocking out both Smad7 and Smurf2. Obviously, since it is not absolutely certain that there does not exist a very small oscillatory regime, this does not mean that our results are a proof that no oscillations can occur without Smad7 and Smurf2, but if this is possible, we do not expect the respective parameter regime to be large and the behavior to be very likely and/or stable.

Apart from the impact on oscillatory behavior we were interested in the impact of feedback components on the concentration of active Smad complexes and on the target gene transcription. Since most of the parameters in the present system are unknown performing a local approach, e.g. an ordinary sensitivity analysis by metabolic control analysis [71] would not lead to conclusive results [72].

Therefore, we used a global approach to analyze the concentration control coefficients for two species of interest that represent the outcome of the signaling event, namely active Smad complexes, as well as target gene transcription by studying their dependency on the synthesis of all feedback species.

Control coefficients in the course of a metabolic control analyses are a specialized form of sensitivity analysis for biochemical systems [73,74]. Sensitivity analyses are employed to determine which parameters are important to and which have a lesser impact on the system's behavior. A sensitivity analysis computes how much a certain system property, for example a steady-state concentration, depends on a specific parameter, for example a kinetic constant. The specialized version, MCA, is very useful as a theoretical framework because it provides a set of summation theorems that explain many system-level properties of biochemical systems. Control coefficients can be defined for any state variable or quantities derived thereof, for example steady-state concentrations and fluxes. Control coefficients measure the response of the system variable in question to infinitesimal changes in the rate of one reaction of the system (for a review see [71]).

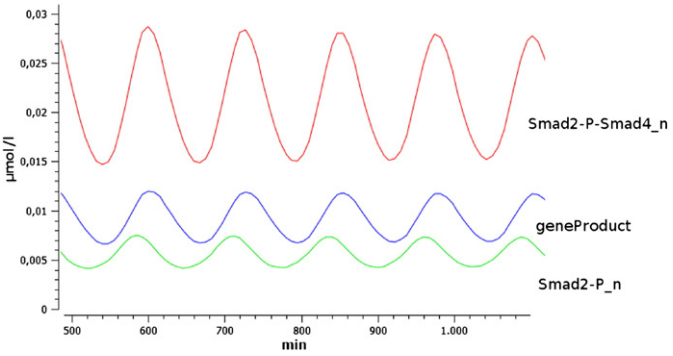

Fig. 2. Predicted oscillatory results for the concentration of phosphorylated Smad2, the active Smad2-Smad4 complexes, and the target gene transcription in the nucleus calculated in Copasi.

It turned out that the best strategy for a global analysis in this specific case was to employ massive random sampling in parameter space. With Copasi, millions of parameter sets were randomly selected and concentration control coefficients for each of them computed. Results for the concentration of the active Smad2 complexes in the nucleus and the target gene transcription are presented in Figs. 3 and 4. The histograms display how many times a concentration control coefficient of a certain magnitude has been found in parameter space, which reflects the ability of the respective feedback species to influence the transcription of those genes that are induced by the signaling cascade. A small coefficient indicates that changing the concentration of the species does not alter gene expression, whereas a large coefficient indicates that there is substantial negative or positive influence onto gene expression. Coefficients equal or larger than one represent a very strong control.

It is of note that the results need to be interpreted very carefully since the distribution of coefficients does not imply by any means that the real values are in the middle of the distribution or similar since the real parameter set is a result of a non-random process (namely evolution). However, the distribution can give insights about minimal and maximal achievable control by a given parameter. Thus, from the histograms (see Figs. 3 and 4) it is quite obvious that Smad7 and the Smurfs have the strongest potential as negative feedback regulator, which coincides with our analysis describing their impact on oscillatory dynamics, mainly driven by feedback loops. Ski and SnoN and to a much lesser extend the other species can also exert both positive, as well as negative control in the system which is interesting by itself. Ski and SnoN have a higher potential for positive control than Smad7 and Smurf1/2, which corresponds to larger positive control coefficients appearing during the random sampling in parameter space. In contrast to this, SARA acts exclusively via positive feedback mechanism. The potential for control indicates that cell type specific responses are dependent on different protein levels resulting in different reaction velocities (parameters in our model) and thus indicating completely different roles of players like Smad7, the Smurfs or Ski/SnoN etc.

Regarding the role of SARA, our model does not capture all interactions described, e.g. the mechanism related to Smad phosphorylation

in the context of TGF-β receptor endocytosis and therefore, it is possible that we underestimate its influence. However, our experimental investigations (see below) point to a minor role of SARA for the system under investigation.

3.3. Experimental results

To evaluate if Smad3 phosphorylation is dependent on its interaction with SARA in AML12 cells, we over-expressed a dominant-negative mutant, lacking the Smad-binding domain [51] in a higher concentration than the endogenous SARA. However, even in the presence of dnSARA we observed a TGF-β mediated phosphorylation of Smad3 (see Fig. 5 A) in AML12 cells. As remaining endogenous Sara could be responsible for Smad3 phosphorylation, we applied RNAi to specifically knock down SARA. In direct comparison with a control siRNA we could validate the stability of our knock down for 72 h, while the control siRNA had no impact onto the expression of SARA (see Fig. 5 B). Remarkably, the knock down of SARA in AML12 cells did neither prevent phosphorylation of Smad3 (see Fig. 5 C) nor block the transcriptional activity of Smad3, measured in a reporter assay (see Fig. 5 D) using Ad(CAGA)9-MLP-Luc [31–33]. These results indicate that at least in our cellular system the interaction between SARA and Smads is dispensable for the R-Smad phosphorylation and are in line with recent findings, showing that Smad phosphorylation is independent of an endocyticstep [75].

Based on the modeling results, we wanted to find evidence for the predicted oscillatory dynamics in real systems. We selected phosphorylated Smad2 because it is predominant in driving TGF-β induced fibrogenesis in the liver [76]. Based on the computational prediction for oscillatory periods between 30 min and 2 h, time-course sampled quantitative immunoblotting was performed with sampling rates of 5 min or 10 min. To detect dynamical behavior, we did not average over different experiments since very small differences between samples would lead to averaging the dynamics out since small differences in the amplitude and especially the timing of

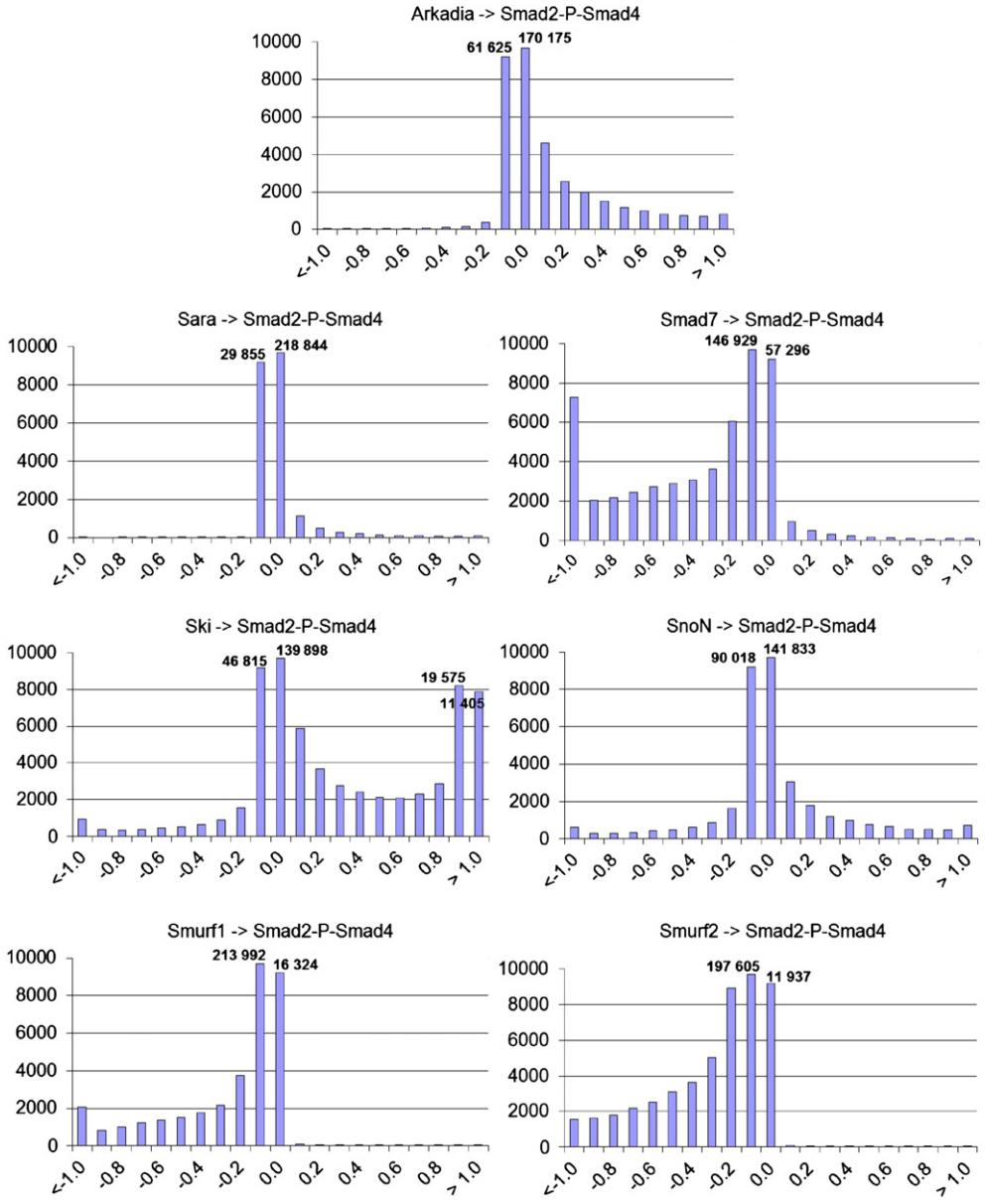

Fig. 3. Histograms of the control coefficients of different production rates of feedback species with respect to the concentration of active Smad2 complexes in the nucleus (e.g. the histogram with the control coefficients of Arkadia with respect to the active pSmad2-Smad4 complex is titled Arkadia -> Smad2-P-Smad4) from the random sampling calculated by Copasi in 500 000 runs. All control coefficients larger than 1 or smaller than −1 are sampled in one column. The x-axis shows the value ranges of the control coefficients between −1 and 1, the y-axis the number of control coefficients that were found in a certain range.

amplitudes would lead to a diminishing of the dynamics when taking averages. Rather, we focused on individual time series. These were analyzed by computing a natural smoothing spline in gnuplot (option acspline with value 0.0005 or 0.001) [77]. However, even though the details of the dynamics varied a bit in between experiments, half of the six experiments performed indicated a dynamic behavior as exemplified by the time series in Fig. 6.

Application of 1 ng/ml TGF-β, highlighted the first peak of Smad2 phosphorylation after 80 min, followed by a decline and a second increase starting after 140 min (see Fig. 6).

To validate our experimental data in cells close to the *in vivo* situation, we chose primary hepatocytes since existing hepatocyte cell lines differ from primary hepatocytes in many relevant aspects [78]. Stimulation of primary mouse hepatocytes with 1 ng/ml TGF-β, caused a rapid phosphorylation of Smad2 with a decline after 120 min, followed by another increase (Fig. 7).

In summary, even though our experimental data highlights the dynamic behavior of TGF-β signaling in primary hepatocytes and an existing hepatocyte cell line with current state-of the art technologies, the data is partially too noisy and the time-series too short to allow conclusions beyond the fact that there is certainly more dynamics involved than just a peak followed by a decline in pSmad as indicated by earlier studies. Longer time series could be extensively analyzed, e.g. for their stochastic content [79,80] or for the nonlinear dynamic properties [81]. It is very difficult to create longer, reliable time-series with the employed technology, since we wanted to load all time-points on a single gel in order to avoid normalization errors resulting from inadvertable differences between gels. Thus the number of data points is restricted. However, we can see that cellular responses in hepatocytes, towards a TGF-β stimulation, are more dynamic than a mere on/off response.

These results show that oscillations are feasible as indicated by our mathematical model for TGF-β mediated signal transduction, but more experimental data, e.g. on the single cell level and/or longer time-series using different technologies are required for verifying this result.

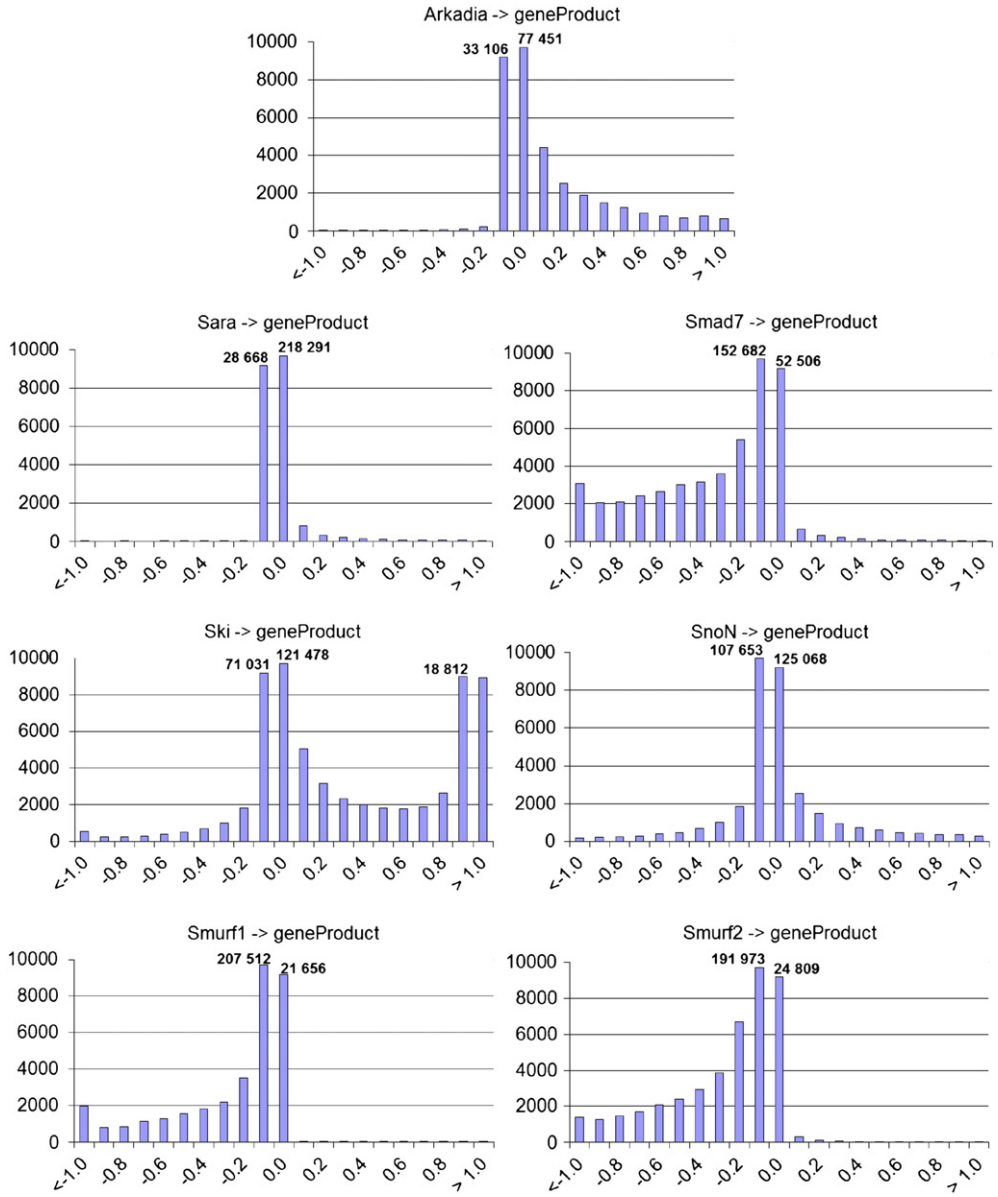

Fig. 4. Histograms of the control coefficients of different production rates of feedback species with respect to transcription based on random sampling calculated by Copasi in 500000 runs (e.g. the histogram with the control coefficients of Arkadia are titled Arkadia -> geneProduct). All control coefficients larger than 1 or smaller than −1 are sampled in one column. The x-axis shows the value ranges of the control coefficients between −1 and 1, the y-axis the number of control coefficients that were found in a certain range.

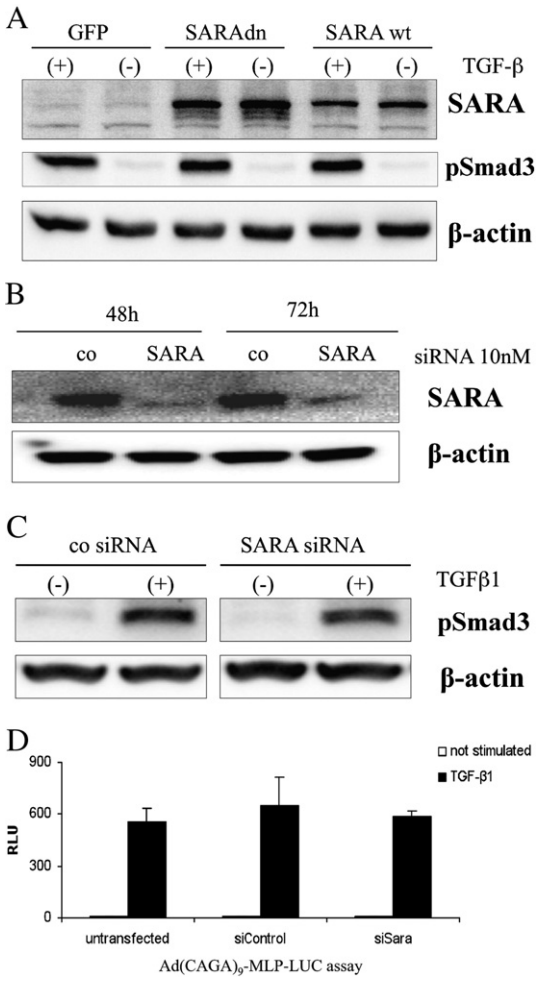

Fig. 5. A. Impact of SARA on TGF-β mediated signal transduction in AML12 hepatocytes. AML12 cells were seeded in 12-well plates and transfected with plasmids as indicated. 16 h after transfection, cells were treated with TGF-β (5 ng/ml) for 30 min. Smad3 phosphorylation is not disturbed upon expression of dnSARA. B. Validation of SARA siRNA knock down was proven by immunoblot expression analysis. AML12 cells were transfected with siRNA as indicated and further cultivated for 48 h or 72 h. Protein lysates were probes with antibodies against SARA and β-actin. C. siRNA knock down of SARA does not prevent TGF-β mediated phosphorylation of Smad3. 48 h after transfection with control siRNAs or SARA siRNA (10 nM), AML12 cells were treated with 5 ng/ml TGF-β for the indicated time points. siRNA knock down of SARA does not diminish phosphorylation of Smad3 by TGF-β. D. Luciferase assay of Ad(CAGA)9-MLP-Luc infected AML12 hepatocytes as a function of SARA RNAi. 2 h after infection AML12 cells were transfected with siRNA (10 nM) and 48 h later, cells were stimulated with TGF-β (5 ng/mL) for 6 h. After lysate preparation, luciferase activity was measured and normalized to protein content. Knock down of SARA has no effect on TGF-β mediated Smad signaling. Independent experiments were done in quadruplicate.

4. Discussion

We presented a complex model of the TGF-β pathway that incorporates main processes including (de)phosphorylation, transport of the signal to the nucleus and several feedback loops. This model is consistent with the following experimental results:

- dimeric TGF-β molecules bind TGF-β-RII and TGF-β-RI dimers [82,83], this complex phosphorylates R-Smads only in the presence of the ligand,
- the rate of the ligand binding to the TGF-βRII increases with the ligand concentration [27],
- in the absence of the signal, R-Smads are mainly in the cytoplasm and Smad4 is equally distributed in nucleus and cytoplasm, but both accumulate in the nucleus upon signal stimulation [44],

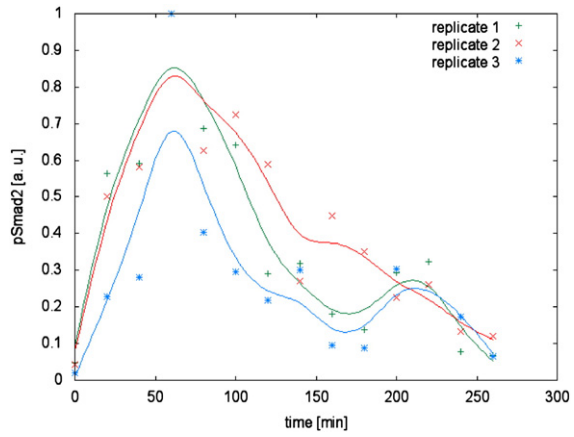

Fig. 6. Time course results of phosphorylated Smad2 in AML12 cells after application of 1 ng/ml TGF-ß concentration. Quantified Western blots were normalized to ß-actin and arbitrary units were calculated in correlation to the maximum value. For the technical replicates three independent Western blot experiments were done. A smoothing spline (smoothing parameter = 0.0005) was fitted to the time courses in gnuplot. The data point at time = 220 min in the experimental technical replicate 3 was excluded from the smoothing spline.

- phosphorylated R-Smads are eliminated faster by phosphatases than by degradation [84],
- Smad7-Smurf complexes are exported faster from the nucleus than Smad7 itself and target receptor complexes for degradation [85,58],
- steady state levels of Smurf2 are sensitive to the amount of Smad7 which stimulates the autocatalytic ubiquitination and subsequent degradation of Smurf2 [58],
- the number of total Smad4 is similar to the level of total Smad2 and Smad3 [24,86].

The results of our computational analysis indicate that oscillations are possible under realistic conditions in this system. They represent a potential mechanism to encode different signals during TGF-β signaling. These findings are underlined by experimental densely sampled time series revealing a more dynamic picture than previously assumed. Similar to BMP induced dynamics [22], the time-scale of the implied dynamics is in the order of one to two hours. Doubtless,

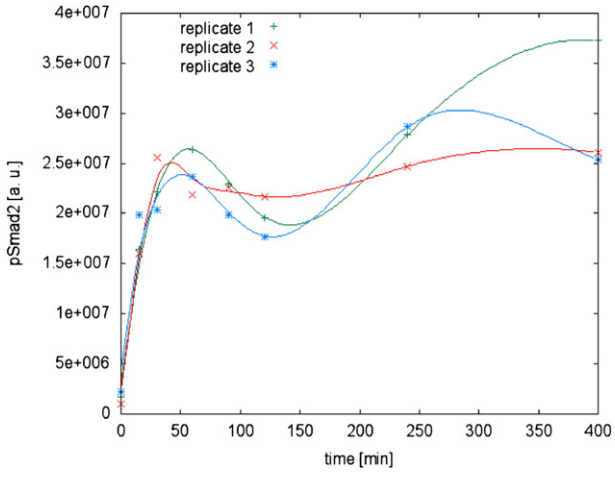

Fig. 7. Time course result of Smad2 phosphorylation in primary hepatocytes. Primary mouse hepatocytes were stimulated with 1 ng/ml TGF-β. Smad2 was immunoprecipitated (IP) from whole cell lysates and phosphorylated Smad2 was determined by subsequent quantitative immunoblotting (IB) based on chemiluminescene detection with the LumiImager system. For data processing, constant amounts of recombinant calibrator proteins SBP-Smad2 were added to the samples prior to immunoprecipitation and loading on SDS-PAGE gels. A smoothing spline (smoothing parameter = 0.001) was fitted to the time courses in gnuplot.

both the data for the AML12 cells as well as the data for the primary mouse hepatocytes are not sufficient to finally prove the existence of oscillations in this system. For a final prove longer time-series would be required, but are currently limited by the available state-of-the-art technologies.

The investigation of the behavior of the model using an open parameter space allowed us to analyze the importance and impact of the different feedback loops in the system in a general manner. This is important since many parameters in the system are to a large extent unknown and different cell types show a different expression pattern of the feedback components in regard of the concentration and the spatio-temporal distribution.

We observed that Smad7 and Smurf2, if present, have the strongest potential to act as negative feedback regulators of the system. The potential dual role predicted for Smad7 and SnoN in TGF-β signaling matches with experimentally observed functions *in vivo*. Increased SnoN expression in tumors, inhibits TGF-β mediated tumor suppressive signaling (for a review see [87]), while at physiological levels it was shown to antagonize TGF-β signaling by sequestration of the Smad proteins [88]. Analyzing the established model suggests that the potential positive role of SnoN is mainly due to the inhibition of the transcription of Smad7 (caused by a complex of Smad4 and SnoN). For Smad7 a functional role as a key regulator of TGF-β mediated signal transduction is well documented. As an agonist of TGF-β mediated signaling, Smad7 promotes initiation of tumor progression, while it can also inhibit metastasis of tumor cells (for a review see [89]). Here, the model shows a potential positive role of Smad7 as a result of the increased degradation of Smurfs which act as negative inhibitors. Thus, in the cases of SnoN and Smad7 it is the relative balance of several feedback loops that renders them either negative or positive feedbacks. This could well be cell type specific.

Sara mainly acts as a potential positive regulator in our model, despite the experimental evidence that Sara is dispensable for the phophorylation of the Smads (see Fig. 5 C and D). However, we do not exclude that in other cellular systems SARA is essential for Smad phosphorylation and will have major functions as positive regulator of the pathway there.

The fact that several feedback loops are able to influence the output of the system either negatively or positively is due to the complexity of the system and opens quite a few possibilities for the cell type dependent regulation. For example, in the case of SnoN it seems that one important interaction is the repression of Smad7 by the Smad4-SnoN complex. This is a positive regulation since the Smad4-SnoN complex competes with the active Smad-complexes for DNA binding either to repress or activate Smad7 which down-regulates the signaling by binding to the receptor complex. Thus, if Smad7 is a dominant regulator, SnoN will likely work as a positive regulator in this cell type. On the other hand, if Smad7 is not dominant, SnoN will easily act as negative feedback regulator.

Information processing in signaling is in general determined by the length and amplitude of a signal. It can also involve oscillatory behavior. For both phenotypes, feedback loops are crucial factors influencing the signals. Therefore, identifying and understanding of involved feedback loops in signaling pathways is of major importance to understand information processing in a certain system and to guide experiments to change the signaling outcome.

It will be interesting to try and manipulate TGF-β signaling such that e.g. oscillatory behavior exhibits large amplitudes and is easier detectable or such that certain feedback loops are strengthened or weakened. Thus, we would expect that shutting down the negative feedback loops will result in a more conventional on/off reply whereas strengthening feedback loops like Smurf2 or Smad7 should increase the nonlinearity of the dynamics. This will enable us to validate the introduced model further.

Acknowledgment

This work was supported by the German Federal Ministry of Education and Research (BMBF) funding priority HepatoSys — "Systems of Life — Systems Biology" (0313082L, 0313078H) as well as "Virtual Liver" (0315764, 0315730) as well as by the Klaus Tschira Foundation.

Appendix A. Supplementary data

Supplementary data to this article can be found online at doi:10.1016/j.bpc.2011.12.003.

References

[1] K. Luo, Ski and SnoN: negative regulators of TGF-β signaling, Current Opinion in Genetics & Development 14 (2004) 65–70.
[2] S.G. Kim, H.-A. Kim, H.-S. Jong, J.-H. Park, N.K. Kim, S.H. Hong, T.-Y. Kim, Y.-J. Bang, The endogenous ratio of Smad2 and Smad3 influences the cytostatic function of Smad3, Molecular Biology of the Cell 16 (2005) 4672–4683.
[3] S. Ross, C. Hill, How the Smads regulate transcription, The International Journal of Biochemistry & Cell Biology 40 (3) (2008) 383–408.
[4] J. Massague, J. Seoane, D. Wotton, Smad transcription factors, Genes & Development 19 (2005) 2783–2810.
[5] C.E. Pierreux, F.J. Nicolas, C.S. Hill, Transforming growth factor β-independent shuttling of Smad4 between the cytoplasm and nucleus, Molecular and Cellular Biology 20 (23) (2000) 9041–9054.
[6] F.J. Nicolas, K.D. Bosscher, B. Schmierer, C.S. Hill, Analysis of Smad nucleocytoplasmic shuttling in living cells, Journal of Cell Science 117 (2004) 4113–4125.
[7] D.M. Bissell, D. Roulot, J. George, Transforming growth factor β and the liver, Hepatology 34 (2001) 859–867.
[8] A.M. Gressner, R. Weiskirchen, K. Breitkopf, S. Dooley, Roles of TGF-beta in hepatic fibrosis, Frontiers in Bioscience 7 (2002) D793–D807.
[9] F.A. Oberhammer, M. Pavelka, S. Sharma, R. Tiefenbacher, A.F. Purchio, W. Bursch, R. Schulte-Hermann, Induction of apoptosis in cultured hepatocytes and in regressing liver by transforming growth factor beta 1, Proceedings of the National Academy of Sciences 89 (1992) 5408–5412.
[10] J.-W. Wu, A.R. Krawitz, J. Chai, W. Li, F. Zhang, K. Luo, Y. Shi, Structural mechanism of Smad4 recognition by the nuclear oncoprotein Ski: insights on Ski-mediated repression of TGF-β signaling, Cell 111 (2002) 357–367.
[11] P. Kavsak, R.K. Rasmussen, C.G. Causing, S. Bonni, H. Zhu, G.H. Thomsen, J.L. Wrana, Smad7 binds to Smurf2 to form an E3 ubiquitin ligase that targets the TGFβ receptor for degradation, Molecular Cell 6 (2000) 1365–1375.
[12] S. Schuster, M. Marhl, T. Höfer, Modelling of simple and complex calcium oscillations — from single-cell responses to intercellular signalling, European Journal of Biochemistry (2002) 1333–1355.
[13] M. Marhl, M. Perca, S. Schuster, Selective regulation of cellular processes via protein cascades acting as band-pass filters for time-limited oscillations, FEBS Letters 579 (2005) 5461–5465.
[14] M. Marhl, M. Perca, S. Schuster, A minimal model for decoding of time-limited Ca2 + oscillations, Biophysical Chemistry 120 (2006) 161–167.
[15] A.Z. Larsen, U. Kummer, Information processing in calcium signal transduction, Lecture Notes in Physics 623 (2003) 153–178.
[16] N. Suzuki, M. Takahata, K. Sato, Oscillatory current responses of olfactory receptor neurons to odorants and computer simulation based on a cyclic AMP transduction model, Chemical Senses 27 (2002) 789–801.
[17] D.E. Nelson, A.E. Ihekwaba, M. Elliott, J.R. Johnson, C.A. Gibney, B.E. Foreman, et al., Oscillations in NF-κB signaling control the dynamics of gene expression, Science 306 (5696) (2004) 704–708 URL, http://dx.doi.org/10.1126/science.1099962.
[18] N.I. Markevich, J.B. Hoek, B.N. Kholodenko, Signaling switches and bistability arising from multisite phosphorylation in protein kinase cascades, The Journal of Cell Biology 164 (3) (2004) 353–359.
[19] R.E. Dolmetsch, K. Xu, R.S. Lewis, Calcium oscillations increase the efficiency and specificity of gene expression, Nature 392 (1998) 933–936.
[20] A. Hoffmann, A. Levchenko, M.L. Scott, D. Baltimore, The I$\kappa B - NF - \kappa$B signaling module: temporal control and selective gene activation, Science 298 (5596) (2002) 1241–1245.
[21] S.G. Park, T. Lee, H.Y. Kang, K. Park, K.-H. Cho, G. Jung, The influence of the signal dynamics of activated form of IKK on NF-κB and anti-apoptotic gene expressions: a systems biology approach, FEBS Letters 580 (2006) 822–830.
[22] S. Yoshiura, T. Ohtsuka, Y. Takenaka, H. Nagahara, K. Yoshikawa, R. Kageyama, Ultradian oscillations of Stat, Smad, and Hes1 expression in response to serum, Proceedings of the National Academy of Sciences 104 (27) (2007) 11292–11297.
[23] J.M.G. Vilar, R. Jansen, C. Sander, Signal processing in the TGF-β superfamily ligand-receptor network, PLoS Computational Biology 2 (1) (2006) 36–45.
[24] D.C. Clarke, M.D. Betterton, X. Liu, Systems theory of Smad signalling, IEE Proceedings — Systems Biology 153 (6) (2006) 412–424.
[25] P. Melke, H. Jonsson, E. Pardali, P. ten Dijke, C. Peterson, A rate equation approach to elucidate the kinetics and robustness of the TGF-β pathway, Biophysical Journal 91 (2006) 4368–4380.
[26] Z. Zi, E. Klipp, Constraint-based modeling and kinetic analysis of the Smad dependent TGF-β signaling pathway, PloS One 9 (2007) e936.

[27] B. Schmierer, C.S. Hill, TGFβ-SMAD signal transduction: molecular specificity and functional flexibility, Nature Reviews Molecular Cell Biology 8 (2007) 970–982.
[28] Z. Zi, Z. Feng, D.A. Chapnick, M. Dahl, D. Deng, E. Klipp, A. Moustakas, X. Liu, Quantitative analysis of transient and sustained transforming growth factor-β signaling dynamics, Molecular Systems Biology 7 (492) (2011).
[29] R.S. Lo, J. Massague, Ubiquitin-dependent degradation of TGF-beta-activated Smad2, Nature Cell Biology 1 (1999) 472–478.
[30] S. Hoops, S. Sahle, R. Gauges, C. Lee, J. Pahle, N. Simus, M. Singhal, L. Xu, P. Mendes, U. Kummer, COPASI a COmplex PAthway SImulator, Bioinformatics 22 (24) (2006) 3067–3074.
[31] S. Dennler, S. Itoh, D. Vivien, P. ten Dijke, S. Huet, J.-M. Gauthier, Direct binding of Smad3 and Smad4 to critical TGFβ-inducible elements in the promoter of human plasminogen activator inhibitor-type 1 gene, The EMBO Journal 17 (1998) 3091–3100.
[32] M. Stopa, D. Anhuf, L. Terstegen, P. Gatsios, A.M. Gressner, S. Dooley, Participation of Smad2, Smad3, and Smad4 in transforming growth factor β (TGF-β)-induced activation of Smad7, The Journal of Biological Chemistry 275 (8) (2000) 29308–29317.
[33] K. Breitkopf, I. Sawitza, J.H. Westhoff, L. Wickert, S. Dooley, A.M. Gressner, Thrombospondin 1 acts as a strong promoter of transforming growth factor beta effects via two distinct mechanisms in hepatic stellate cells, Gut 54 (2005) 673–681.
[34] U. Klingmüller, A. Bauer, Primary mouse hepatocytes for systems biology approaches: a standardized in vitro system for modelling of signal transduction pathways, Systems Biology 153 (2006) 433–447.
[35] E. Wiercinska, L. Wickert, B. Denecke, M.H. Said, J. Hamzavi, A.M. Gressner, M. Thorikay, P.T. Dijke, P.R. Mertens, K. Breitkopf, S. Dooley, Id1 is a critical mediator in TGF-β-induced transdifferentiation of rat hepatic stellate cells, Hepatology 43 (2006) 1032–1041.
[36] M. Schilling, T. Maiwald, S. Bohl, M. Kollmann, C. Kreutz, J. Timmer, U. Klingmüller, Computational processing and error reduction strategies for standardized quantitative data in biological networks, FEBS Journal 272 (2005) 6400–6411.
[37] C. Li, M. D. nd N Rodriguez, H. Dharuri, L. Endler, V. Chelliah, L. Li, E. He, A. Henry, M. Stefan, J. Snoep, M. Hucka, N.L. Novère, C. Laibe, BioModels Database: An enhanced, curated and annotated resource for published quantitative kinetic models, BMC Systems Biology 4 (92) (2010).
[38] S. Dennler, S. Huet, J.-M. Gauthier, A short amino-acid sequence in MH1 domain is responsible for functional differences between Smad2 and Smad3, Oncogene 18 (1999) 1643–1648.
[39] K.A. Brown, J.A. Pietenpol, H.L. Moses, A tale of two proteins: differential roles and regulation of Smad2 and Smad3 in TGF-β signaling, Journal of Cellular Biochemistry 101 (4) (2007) 9–33.
[40] J.-W. Wu, D.R. Fairman, J.P. Dagger, Y.S. Dagger, Formation of a stable heterodimer between Smad2 and Smad4, Journal of Biological Chemistry 276 (2001) 20688–20694.
[41] B.M. Chacko, B.Y. Qin, A. Tiwari, G. Shi, S. Lam, L.J. Hayward, M. de Caestecker, K. Lin, Structural basis of heteromeric Smad protein assembly in TGF-β signaling, Molecular Cell 15 (2004) 813–823.
[42] L. Zawel, J.L. Dai, P. Buckhaults, S. Zhou, K.W. Kinzler, B. Vogelstein, S.E. Kern, Human Smad3 and Smad4 are sequence-specific transcription activators, Molecular Cell 1 (1998) 611–617.
[43] H.B. Chen, J.G. Rud, K. Lin, L. Xu, Nuclear targeting of transforming growth factor-β-activated Smad complexes, The Journal of Biological Chemistry 280 (22) (2005) 21329–21336.
[44] B. Schmierer, C.S. Hill, Kinetic analysis of Smad nucleocytoplasmic shuttling reveals a mechanism for transforming growth factor β — dependent nuclear accumulation of Smads, Molecular and Cellular Biology 25 (22) (2005) 9845–9858.
[45] X. Lin, X. Duan, Y.-Y. Liang, Y. Su, K.H. Wrighton, J. Long, M. Hu, C.M. Davis, J. Wang, F.C. Brunicardi, Y. Shi, Y.-G. Chen, A. Meng, X.-H. Feng, PPM1A functions as a Smad phosphatase to terminate TGFβ signaling, Cell 125 (2006) 915–928.
[46] C.E. Runyan, H.W. Schnaper, A.-C. Poncelet, The role of internalization in transforming growth factor 1-induced Smad2 association with Smad anchor for receptor activation (SARA) and Smad2-dependent signaling in human mesangial cells, The Journal of Biological Chemistry 280 (9) (2005) 8300–8308.
[47] G.M.D. Guglielmo, C.L. Roy, A.F. Goodfellow, J.L. Wrana, Distinct endocytic pathways regulate TGF-β receptor signalling and turnover, Nature Cell Biology 54 (2003) 410–422.
[48] L. Xu, Y.-G. Chen, J. Massagué, The nuclear import function of Smad2 is masked by SARA and unmasked by TGFβ-dependent phosphorylation, Nature Cell Biology 2 (2000) 559–562.
[49] D. Goto, H. Nakajima, Y. Mori, K. Kurasawa, N. Kitamura, I. Iwamoto, Interaction between Smad anchor for receptor activation and Smad3 is not essential for TGF-β/Smad3-mediated signaling, Biochemical and Biophysical Research Communications 281 (2001) 1100–1105.
[50] Z. Lu, J.T. Murray, W. Luo, H. Li, X. Wu, H. Xu, J.M. Backer, Y.-G. Chen, Transforming growth factor β activates Smad2 in the absence of receptor endocytosis, Journal of Biological Chemistry 277 (2002) 29363–29368.
[51] T. Tsukazaki, T.A. Chiang, A.F. Davison, L. Attisano, J.L. Wrana, SARA, a FYVE domain protein that recruits Smad2 to the TGFβ receptor, Cell 95 (1998) 779–791.
[52] S. Hayes, A. Chawla, S. Corvera, TGFβ receptor internalization into EEA1-enriched early endosomes: role in signaling to Smad2, The Journal of Cell Biology 158 (7) (2002) 1239–1249.
[53] G. von Gersdorff, K. Susztak, F. Rezvani, M. Bitzer, D. Liang, E.P. Boettinger, Smad3 and Smad4 mediate transcriptional activation of the human Smad7 promoter by transforming growth factor β, The Journal of Biological Chemistry 275 (15) (2000) 11320–11326.
[54] H. Hayashi, S. Abdollah, Y. Qiu, J. Cai, Y.-Y. Xu, B.W. Grinnell, M.A. Richardson, J.N. Topper, J. Michael, A. Gimbrone, J.L. Wrana, D. Falb, The MAD-related protein Smad7 associates with the TGFβ receptor and functions as an antagonist of TGFβ Signaling, Cell 89 (1997) 1165–1173.
[55] A. Nakao, T. Imamura, S. Souchelnytskyi, M. Kawabata, A. Ishisaki, E. Oeda, K. Tamaki, J.-I. Hanai, C.-H. Heldin, K. Miyazono, P. ten Dijke, TGF-β receptor-mediated signalling through Smad2, Smad3 and Smad4, The EMBO Journal 16 (17) (1997) 5353–5362.
[56] V.R. Briones, S. Chen, A.T. Riegel, R.J. Lechleider, Mechanism of Fibroblast growth factor-binding protein repression by TGF-β, Biochemical and Biophysical Research Communications 345 (2006) 595–601.
[57] T. Ebisawa, M. Fukuchi, G. Murakami, T. Chiba, K. Tanaka, T. Imamura, K. Miyazono, Smurf1 interacts with transforming growth factor-β Type I receptor through Smad7 and induces receptor degradation, Journal of Biological Chemistry 276 (2001) 12477–12480.
[58] A.A. Ogunjimi, D.J. Briant, N. Pece-Barbara, C.L. Roy, G.M.D. Guglielmo, P. Kavsak, R.K. Rasmussen, B.T. Seet, F. Sicheri, J.L. Wrana, Regulation of Smurf2 ubiquitin ligase activity by anchoring the E2 to the HECT domain, Molecular Cell 19 (2005) 297–308.
[59] M. Fukuchi, T. Imamura, T. Chiba, T. Ebisawa, M. Kawabata, K. Tanaka, K. Miyazono, Ligand-dependent degradation of Smad3 by a ubiquitin ligase complex of ROC1 and associated proteins, Molecular Biology of the Cell 12 (2001) 1431–1443.
[60] S.L. Stroschein, W. Wang, S. Zhou, Q. Zhou, K. Luo, Negative feedback regulation of TGF-β signaling by the SnoN oncoprotein, Science 286 (1999) 771–774.
[61] X. Liu, Y. Sun, R.A. Weinberg, H.F. Lodish, Ski/Sno and TGF-β signaling, Cytokine & Growth Factor Reviews 12 (2001) 1–8.
[62] S. Bonni, H.-R. Wang, C.G. Causing, P. Kavsak, S.L. Stroschein, K. Luo, J.L. Wrana, TGF-beta induces assembly of a Smad2-Smurf2 ubiquitin ligase complex that targets SnoN for degradation, Nature Cell Biology 3 (2001) 587–595.
[63] R. Tan, W. He, X. Lin, L. P. P. Kiss, Y. Liu, Smad ubiquitination regulatory factor-2 in the fibrotic kidney: regulation, target specificity and functional implication., American journal of physiology. Renal physiologydoi:http://dx.doi.org/10.1152/ajprenal.00323.2007. URL http://dx.doi.org/10.1152/ajprenal.00323.2007.
[64] J. He, S.B. Tegen, A.R. Krawitz, G.S. Martin, K. Luo, The transforming activity of Ski and SnoN is dependent on their ability to repress the activity of Smad proteins, The Journal of Biological Chemistry 278 (33) (2003) 30540–30547.
[65] L. Levy, M. Howell, D. Das, S. Harkin, V. Episkopou, C.S. Hill, Arkadia activates Smad3/Smad4-dependent transcription by triggering signal-induced SnoN degradation, Molecular and Cellular Biology 27 (2007) 6068–6083.
[66] Y. Nagano, K.J. Mavrakis, K.L. Lee, T. Fujii, D. Koinuma, H. Sase, K. Yuki, K. Isogaya, M. Saitoh, T. Imamura, V. Episkopou, K. Miyazono, K. Miyazawa, Arkadia induces degradation of SnoN and c-Ski to enhance transforming growth factor-β signaling, Journal of Biological Chemistry 282 (2007) 20492–20501.
[67] Y. Inoue, T. Imamura, Regulation of TGF-β family signaling by E3 ubiquitin ligases, Cancer Science 99 (2008) 2107–2112.
[68] R.C. Eberhart, J. Kennedy, A new optimizer using particle swarm theory, 6th Int. Symp. on Micromachine and Human Science, Nagoya, Japan, 1995, pp. 39–45.
[69] M. Mitchell, An Introduction to Genetic Algorithms, MIT Press, Boston, MA, 1995.
[70] H.G. Beyer, The Theory of Evolution Strategies, Springer, Berlin, Germany, 2001.
[71] M. Cascante, L.G. Boros, B. Comin-Anduix, P. de Atauri, J.J. Centelles, P.W.-N. Lee, Metabolic control analysis in drug discovery and disease, Nature Biotechnology 20 (2001) 243–249.
[72] S. Sahle, P. Mendes, S. Hoops, U. Kummer, A new strategy for assessing sensitivities in biochemical models, Philosophical Transactions of the Royal Society of London, Series A 366 (2008) 3619–3631.
[73] H. Kacser, J.A. Burns, The control of flux, Symposia of the Society for Experimental Biology 27 (1973) 65–104.
[74] R. Heinrich, T.A. Rapoport, A linear steady-state treatment of enzymatic chains. General properties, control and effector strength, European Journal of Biochemistry 42 (1974) 89–95.
[75] C. Meyer, P. Godoy, A. Bachmann, Y. Liu, D. Barzan, I. Ilkavets, P. Maier, C. Herskind, J.G. Hengstler, S. Dooley, Distinct role of endocytosis for Smad and non-Smad TGF-β signaling regulation in hepatocytes, Journal of Hepatology 55 (2) (2011) 369–378.
[76] B. Schnabl, Y.O. Kweon, J.P. Frederick, X.-F. Wang, R.A. Rippe, D.A. Brenner, The role of Smad3 in mediating mouse hepatic stellate cell activation, Hepatology 34 (1) (2001) 89–100.
[77] P.K. Janert, Gnuplot in Action — Understanding Data with Graphs, Manning Publications, 2009.
[78] C. Pan, C. Kumar, S. Bohl, U. Klingmueller, M. Mann, Comparative proteomic phenotyping of cell lines and primary cells to assess preservation of cell type specific functions, Molecular & Cellular Proteomics 8 (3) (2008) 443–450.
[79] M. Perc, A.K. Green, C.J. Dixon, M. Marhl, Establishing the stochastic nature of intracellular calcium oscillations from experimental data, Biophysical Chemistry 132 (2008) 33–38.
[80] M. Perc, M. Rupnik, M. Gosak, M. Marhl, Prevalence of stochasticity in experimentally observed responses of pancreatic acinar cells to acetylcholine, Chaos (2009) 037113.
[81] L. Glass, D. Kaplan, Time series analysis of complex dynamics in physiology and medicine, Medical Progress through Technology 19 (1993) 115–128.
[82] R.A. Rahimi, E.B. Leof, TGF-β signaling: a tale of two responses, Journal of Cellular Biochemistry 102 (2007) 593–608.
[83] K. Luo, H.F. Lodish, Positive and negative regulation of type II TGF-β receptor signal transduction by autophosphorylation on multiple serine residues, The EMBO Journal 16 (8) (1997) 1970–1981.
[84] G.J. Inman, F.J. Nicolas, C.S. Hill, Nucleocytoplasmic shuttling of Smads 2, 3, and 4 permits sensing of TGF-β receptor activity, Molecular Cell 10 (2002) 283–294.
[85] Y. Tajima, K. Goto, M. Yoshida, K. Shinomiya, T. Sekimoto, Y. Yoneda, K. Miyazono, T. Imamura, Chromosomal region maintenance 1 (CRM1)-dependent nuclear

export of Smad ubiquitin regulatory factor 1 (Smurf1) is essential for negative regulation of transforming growth factor-β signaling by Smad7, Journal of Biological Chemistry 278 (12) (2003) 10716–10721.
[86] B. Schmierer, A.L. Tournier, P.A. Bates, C.S. Hill, Mathematical modeling identifies Smad nucleocytoplasmic shuttling as a dynamic signal-interpreting system, PNAS 105 (18) (2008) 6608–6613.
[87] S. Lamouille, R. Derynck, Oncogene and tumour suppressor: the two faces of SnoN, EMBO Journal 28 (2009) 3459–3460.
[88] A.R. Krakowski, J. Laboureau, A. Mauviel, M.J. Bissell, K. Luo, Cytoplasmic snon in normal tissues and nonmalignant cells antagonizes tgf-beta signaling by sequestration of the smad proteins, PNAS 102 (35) (2005) 12437–12442.
[89] X. Yan, Y.-G. Chen, Smad7: not only a regulator, but also a cross-talk mediator of TGF-β signalling, Biochemical Journal 434 (2011) 1–10.
[90] W. Chen, S.S. Lam, H. Srinath, C.A. Schiffer, J. William, E. Royer, K. Lin, Competition between Ski and CREB-binding protein for binding to Smad proteins in transforming growth factor-β Signaling, Journal of Biological Chemistry 282 (2007) 11365–11376.